# Stochastic Superparameterization and multiscale filtering of turbulent tracers

Yoonsang Lee, Andrew J Majda, Di Qi

Center for Atmosphere Ocean Science (CAOS)
Courant Institute of Mathematical Sciences (CIMS)
New York University

Former collaborator
I. Grooms

The 7th EnKF Data Assimilation Workshop
May 25, 2016

Main reference

- Y. Lee, A.J. Majda, and D. Qi, **Stochastic superparameterization and multiscale data assimilation of turbulent tracers**, submitted to Journal of Computational Physics

Stochastic superparameterization

- A.J. Majda, I. Grooms, **New perspectives on superparameterization for geophysical turbulence**, J. Comp. Phy., 271, 60–77, 2014

Multiscale data assimilation

- Y. Lee and A.J. Majda, **Multiscale methods for data assimilation in turbulent systems**, SIAM MMS 13(2), 691-173, 2015

# Turbulent tracers

$$\frac{\partial T}{\partial t} + \mathbf{v} \cdot \nabla T = \mathcal{D} T \qquad (1)$$

$T(\mathbf{x}, t)$ : concentration of the tracer immersed in the fluid
$\mathbf{v}(\mathbf{x}, t)$ : velocity field
$\mathcal{D}$ : scale-selective linear dissipation operator

- spread of $CO_2$ in atmosphere, pollutants in environmental science
- interaction of many complex factors in $\mathbf{v}$ invoke rare fluctuations
- computationally expensive

**Goal of this talk** : data assimilation of turbulent tracers using

- Reduced-order (coarse resolution) forecast model : stochastic superparameterization
  - coarse-scale (large-scale) prediction
- Multiscale data assimilation method
  - mixed contributions from the resolved large-scales and unresolved small-scales
  - Estimation of large-scale dynamics using mixed observations

cf. data assimilation using superparameterization with large-scale observation - Harlim and Majda, MMS 2013

# Turbulent flow : two-layer quasigeostrophic equation

$$
\begin{aligned}
\partial_t q_1 &= -\tilde{\mathbf{v}}_1 \cdot \nabla q_1 - \partial_x q_1 - (k_\beta^2 + k_d^2)\tilde{v}_1 - \nu \Delta^4 q_1, \\
\partial_t q_2 &= -\tilde{\mathbf{v}}_2 \cdot \nabla q_2 + \partial_x q_2 - (k_\beta^2 - k_d^2)\tilde{v}_2 - r\Delta\psi_2 - \nu \Delta^4 q_2, \\
q_1 &= \Delta\psi_1 + \frac{k_d^2}{2}(\psi_2 - \psi_1), \\
q_2 &= \Delta\psi_2 - \frac{k_d^2}{2}(\psi_2 - \psi_1)
\end{aligned}
\tag{2}
$$

- $q_j$ : potential vorticity in the upper ($j = 1$) and lower ($j = 2$) layers
- $r$ : linear Ekman drag coefficient at the bottom layer
- $\nu$ : hyperviscosity
- $k_d$ : deformation wavenumber
- $k_\beta$ : nondimensionalized variation of the vertical projection of Coriolis frequency with latitude
- $\mathbf{v}_j = (-\partial_y \psi_j + (-1)^{j-1}, \partial_x \psi_j), \quad j = 1, 2$

# Turbulent tracer with a mean gradient

- a tracer field with a large-scale mean tracer gradient (Majda and Gershgorin Proc. Roy. Soc. '13),
  $T_j = T_j' + a_j x + b_j y$

$$\partial_t T_j' + \mathbf{v}_j \cdot \nabla T_j' = -a_j(\tilde{u}_j + (-1)^{j-1}) - b_j \tilde{v}_j - \kappa \Delta^4 T_j' + F_j^{ext} \quad (3)$$

  with an external forcing $F_j^{ext} = a_j(-1)^{j-1}$
- $T_j' = a_j \chi_j + b_j \phi_j$ where

$$\text{along-jet}: \ \partial_t \chi_j + \mathbf{v}_j \cdot \nabla \chi_j = -\tilde{u}_j - \kappa \Delta^4 \chi_j, \quad (4)$$

$$\text{across-jet}: \ \partial_t \phi_j + \mathbf{v}_j \cdot \nabla \phi_j = -\tilde{v}_j - \kappa \Delta^4 \phi_j. \quad (5)$$

- tracer variance is maintained by the zonal and meridional velocity components

# Test regimes and reference simulation results

- High, mid and low latitude cases

$$\begin{aligned}
\text{High}: &\quad k_\beta = 0 \text{ and } r = 8,\\
\text{Mid}: &\quad k_\beta^2 = k_d^2/4 \text{ and } r = 2,\\
\text{Low}: &\quad k_\beta^2 = k_d^2/2 \text{ and } r = 0.5,
\end{aligned}$$

  $k_d = 25$, $\nu = 1.28 \times 10^{-15}$
- $256 \times 256$ resolution, pseudo-spectral code, semi-implicit Runge-Kutta method with a time step $2 \times 10^{-5}$

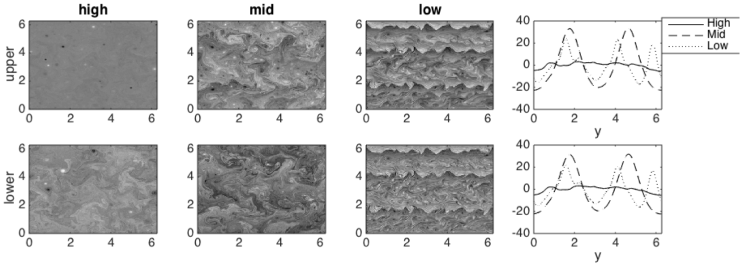


Figure: Snapshots of potential vorticities $q_j, j = 1, 2$. The fourth column is the temporally and zonally averaged zonal velocity.

Growth rates of the unstable modes with $k_y = 0$

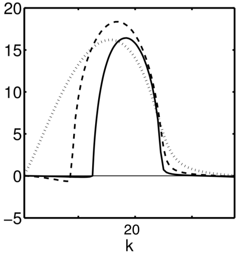


Kinetic energy (KE) and available potential energy (APE) spectra

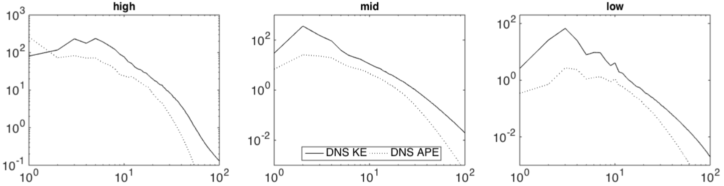

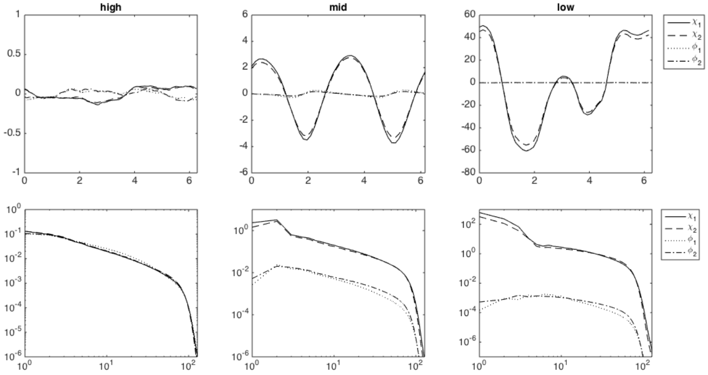


Figure: (Top) Temporally and zonally averaged along-jet $\chi_j, j = 1, 2$, and across-jet, $\phi_j, j = 1, 2$ tracer fields. (Bottom) Tracer variance spectra about the mean.

Probability distribution of the along-jet ($\chi'_j$) and across-jet ($\phi'_j$) tracer fields around the mean

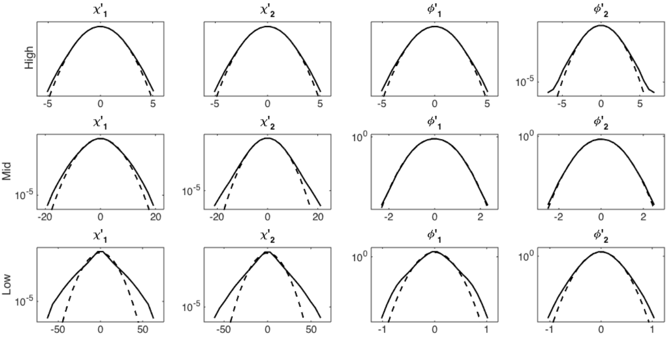


dashed line : Gaussian fit

# Stochastic superparameterization

Seamless multiscale method for the parameterization of the unresolved sub-grid scales

- Apply a low-pass spatial filter denoted by $\bar{(\cdot)}$

$$\begin{aligned}\partial_t \bar{q}_1 &= -\bar{\tilde{\mathbf{v}}}_1 \cdot \nabla \bar{q}_1 - \overline{\tilde{\mathbf{v}}_1 \cdot \nabla q_1} - \partial_x \bar{q}_1 - (k_\beta^2 + k_d^2)\bar{v}_1 - \nu \Delta^2 \bar{\omega}_1,\\ \partial_t \bar{q}_2 &= -\bar{\tilde{\mathbf{v}}}_2 \cdot \nabla \bar{q}_2 - \overline{\tilde{\mathbf{v}}_2 \cdot \nabla q_2} + \partial_x \bar{q}_2 - (k_\beta^2 - k_d^2)\bar{v}_2 - r\Delta\bar{\psi}_2 \\ &\quad - \nu \Delta^2 \bar{\omega}_2\end{aligned} \tag{6}$$

where $\overline{\omega_j} = \Delta\overline{\psi_j}$ is the relative vorticity.

- Not closed under the large-scale variables
- Net transfer of kinetic energy from small to large scales

# Modeling of eddy terms

Majda and Grooms JCP 2014

- randomly oriented plane waves
- conditional Gaussian closure; replace nonlinear terms in eddy equations by additive stochastic forcing and linear deterministic damping conditional to large-scale variables
- quasilinear eddy equations solved in formally infinite embedded domains; no scale-gap
- interaction between large- and small-scale variables are maintained by the conditional dependence of eddy equations on the large-scale variables

Total kinetic energy and available potential energy spectra

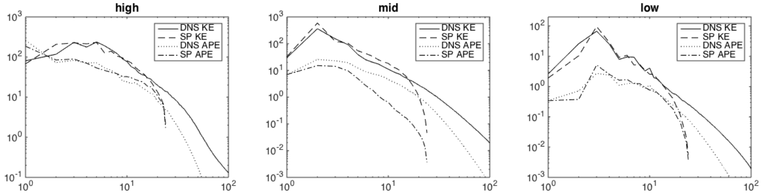


Temporally and zonally averaged zonal velocity components for the mid (left two) and low (right two) latitude cases

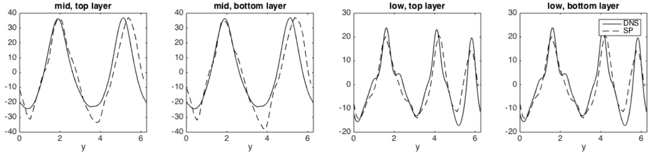

# Reduced-order model for tracer fields

- obtained by adding additional diffusion, while tracers are advected by large-scale velocity fields
- jets act as barriers to meridional tracer transport. The transport in the along-jet direction becomes stronger than the one in the across-jet direction
- The eddy diffusion is modeled by an anisotropic biharmonic diffusion $-\kappa_{aniso}\mathcal{D}^2_{aniso}$ where $\kappa_{aniso}$ is a diffusion coefficient and the linear dissipation $\mathcal{D}_{aniso}$ is given by

$$\mathcal{D}_{aniso} = \alpha\partial_{xx} + \partial_{yy} \tag{7}$$

with a tunable parameter $\alpha$ controlling the anisotropy of the diffusion.

# Tracer variance spectra of truth (DNS) and SP

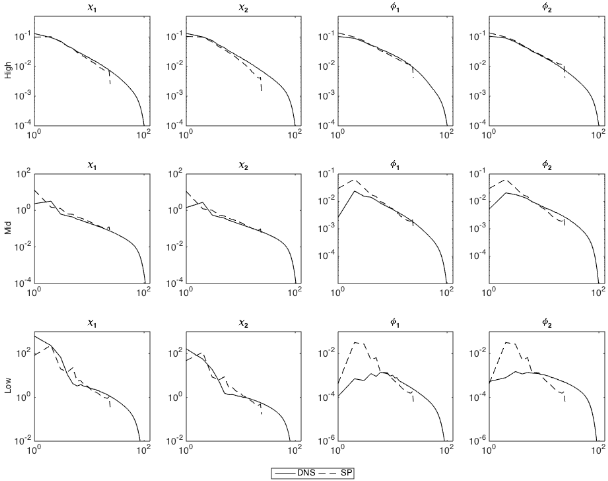


$\kappa_{aniso}$ = 1.1E-3 (high), 3.0E-4 (mid), 1.0E-4 (low)
$\alpha$ = 1.0 (high), 1.1 (mid), 1.4 (low)

Temporally and zonally averaged tracer mean of truth (DNS) and SP

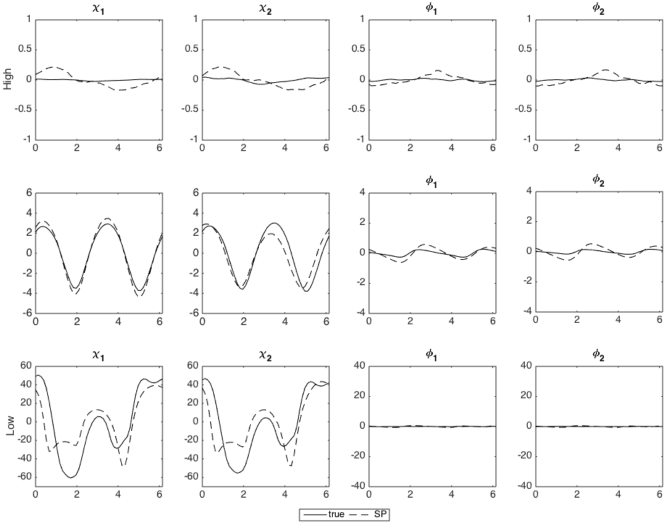

Low latitude case : Probability distributions of fluctuating tracer fields around the mean state

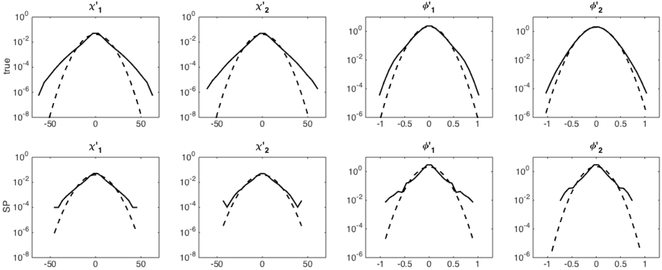

# Multiscale data assimilation

- Reduced-order forecast provides prior information only for the resolved scales
- Observation contain contributions both from the resolved and unresolved scales
- Use multiscale data assimilation methods to achieve accurate estimation of the large-scale statistics

- For a tracer field $c$

$$c = (\bar{c}, c') \tag{8}$$

$\bar{c}$ and $c'$ represent the resolved and unresolved scale components respectively

- For simplicity consider linearly related observation $w$

$$w = \bar{G}\bar{c} + G'c' + \xi_o \tag{9}$$

$\bar{G}$ and $G'$ are observation matrix corresponding to the resolved and unresolved scales. $\xi_o$ is Gaussian with zero-mean and a covariance $r_o I$

- Full state $c = (\overline{c}, c')$ is assumed to be (conditionally) Gaussian with a covariance $R$ in the following form

$$R = \begin{pmatrix} \bar{R} & \\ & R'(\overline{c}) \end{pmatrix} \qquad (10)$$

- Small-scale covariance conditional to the large scale variable; non-trivial and non-Gaussian statistics
- no cross correlation between the resolved and unresolved scales
- It can be shown that for zero-mean $c'$ which is Gaussian conditional to $\overline{c}$ there is no correlation between $\overline{c}$ and $c'$[1]

[1] Grooms, Lee & Majda, JCP 2014

Apply Bayes' theorem to the prior forecast state $c^f$ with a prior covariance $R^f$ yields

$$\begin{aligned}
\bar{c}^a &= \bar{c}^f + \bar{K}(w - \bar{G}\bar{c}) \\
\bar{K} &= \bar{R}^f \bar{G}^T (\bar{G}\bar{R}^f \bar{G}^T + G' R'^f G'^T + r_o I)^{-1} \\
\bar{R}^a &= (I - \bar{K}\bar{G})\bar{R}^f
\end{aligned} \tag{11}$$

- standard Kalman update formula for $\bar{c}$ with the same observation $w$ and an increased observation variance $G' R' G'^T + r_o I$ is added to the Kalman gain matrix due to the effect from the unresolved scales
- Use climatological variance of the unresolved scales; diagonal covariance matrix for the unresolved scales
- Straightforward to apply standard ensemble data assimilation methods to update $\bar{c}$

# Covariance inflation

- Reduced-order forecast model is an imperfect model and thus model errors are unavoidable in the data assimilation
- Almost all ensemble members may collapse to one single ensemble value with little variance
- Covariance inflation is an effective remedy increasing the uncertainty in the forecast model
- We use additional covariance inflation which adds additional noise to the prior ensemble members

$$\bar{c}^k \leftarrow \bar{c}^k + \xi_a \tag{12}$$

$\xi_a$ is Gaussian with zero mean and a variance $r_a^2$ and i.i.d in space and time

# Filtering results

- True signal : DNS with $256 \times 256$ resolution for both layers, time step $2 \times 10^{-5}$
- Forecast : SP and eddy diffusion with $48 \times 48$ resolution, time step $10^{-4}$ (250 times less expensive than DNS)
- Large-scale variable is defined as the Fourier truncated variable with a cutoff wavenumber $k = 24$
- Observation : upper layer tracer field on the $48 \times 48$ grid
- Raw observation error : 5% of the upper layer tracer field variance
- Observation interval : 0.01, comparable to or shorter than the decorrelation times

- Effective observation error

$$\sqrt{\text{raw obs error variance} + \text{small-scale variance}} \tag{13}$$

- 50 ensemble members using EAKF
- run 500 cycles and use the last 300 cycles to measure filter performance

$$\text{time-averaged RMS error} = \frac{1}{M - m_0} \sum_{m=m_0+1}^{M} \|c_m^a - c_m^t\| \tag{14}$$

and

$$\text{time-averaged PC} = \frac{1}{M - m_0} \sum_{m=m_0+1}^{M} \frac{\sum_{x_i} c_m^a c_m^t}{\|c_m^a\| \|c_m^t\|} \tag{15}$$

where $\| \cdot \|$ represents the $l_2$ norm on the coarse grid points $\{x_i\}$, $m_0 = 200$ and $M = 500$.

| **High** | without inflation | with inflation | Effect obs error | stationary std |
|---|---|---|---|---|
| $\chi_1$ | 1.56 (0.01) | 0.51 (0.87) | 0.60 | 1.04 |
| $\chi_2$ | 1.61 (-0.01) | 0.92 (0.65) | N/A | 1.06 |
| $\phi_1$ | 1.65 (-0.00) | 0.55 (0.88) | 0.62 | 1.16 |
| $\phi_2$ | 1.70 (0.00) | 0.99 (0.57) | N/A | 1.10 |
| **Mid** | without inflation | with inflation | Effect obs error | stationary std |
| $\chi_1$ | 4.55 (0.15) | 1.75 (0.90) | 1.95 | 4.19 |
| $\chi_2$ | 4.21 (0.13) | 2.83 (0.77) | N/A | 3.93 |
| $\phi_1$ | 0.91 (0.11) | 0.28 (0.88) | 0.29 | 0.55 |
| $\phi_2$ | 0.85 (0.10) | 0.52 (0.60) | N/A | 0.60 |
| **Low** | without inflation | with inflation | Effect obs error | stationary std |
| $\chi_1$ | 25 (0.65) | 6.77 (0.98) | 10.24 | 37.62 |
| $\chi_2$ | 23 (0.61) | 17.1 (0.96) | N/A | 21.50 |
| $\phi_1$ | 0.18 (0.08) | 0.10 (0.86) | 0.10 | 0.18 |
| $\phi_2$ | 0.29 (-0.01) | 0.68 (0.57) | N/A | 0.24 |

Table: RMS errors and pattern correlations in parenthesis of the posterior mean in the estimation of the large-scale variables

# Temporally and zonally averaged tracer mean of true and filtered signals

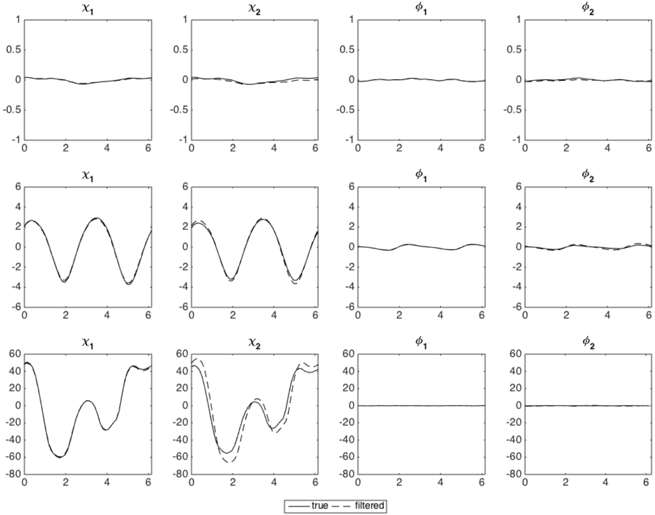

## Low latitude case : Probability distributions of fluctuating tracer fields around the mean state

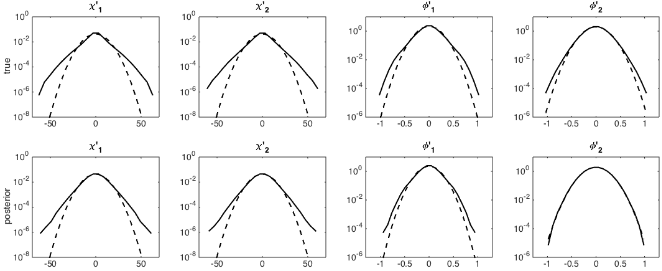

# Conclusions

- Coarse resolution forecast model for turbulent flows with significantly reduced computational cost; 250 times cheaper than full resolution model
- Multiscale ensemble filtering; skillfull filtering results and recovery of fat-tail PDFs

Catastrophic filter divergence

- Y. Lee, A.J. Majda, D. Qi, *Preventing catastrophic filter divergence using adaptive additive inflation for baroclinic turbulence*, submitted to Monthly Weather Review
- X. Tong, A.J. Majda, D. Kelly, *Nonlinear stability of the ensemble Kalman filter with adaptive covariance inflation*, Comm. Math. Sci 14(5), 1283-1313, 2016
- X. Tong, A.J. Majda, D. Kelly, *Nonlinear stability and ergodicity of ensemble based Kalman filters*, Nonlinearity, 29(2), 2016

Thanks for your attention